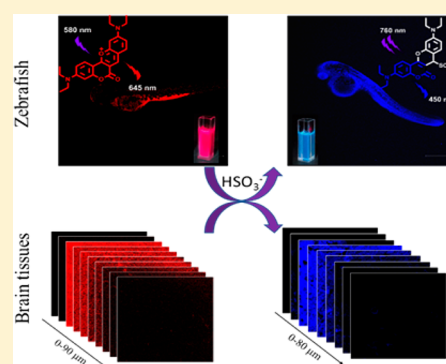# Two-Photon and Deep-Red Emission Ratiometric Fluorescent Probe with a Large Emission Shift and Signal Ratios for Sulfur Dioxide: Ultrafast Response and Applications in Living Cells, Brain Tissues, and Zebrafishes

Yanyan Ma, Yonghe Tang, Yuping Zhao, Shiying Gao, and Weiying Lin*

Institute of Fluorescent Probes for Biological Imaging, School of Chemistry and Chemical Engineering, School of Materials Science and Engineering, University of Jinan, Jinan, Shandong 250022, P.R. China

S Supporting Information

ABSTRACT: Sulfur dioxide (SO_2) is a dangerous environmental pollutant. Excessive intake of it may cause some respiratory diseases and even lung cancer. The development of effective methods for detection of SO_2 is of great importance for the environment and physiology. Herein, we have designed and synthesized a novel two-photon (TP) and deep-red emission ratiometric fluorescent probe (**CP**) for detection of SO_2. Notably, the novel probe **CP** exhibited ultrafast response to SO_2 in less than 5 s and displayed a great emission shift (195 nm) and a large emission signal ratio variation (enhancement from 0.1347 to 100.14). In addition, the unique probe was successfully employed for imaging SO_2 not only in the mitochondria of living cells but also in brain tissues and zebrafishes.

Sulfur dioxide (SO_2) has been recognized as a serious environmental pollutant over the past few years,[1,2] and its derivatives (sulfite and bisulfite) have been used as preservatives and antioxidants in the food, wine, and pharmaceutical industry.[3−5] Epidemiological studies showed that excessive intake of SO_2 or/and its derivatives may cause respiratory diseases[6,7] (e.g., asthma, emphysema, chronic bronchitis), neurological disorders[8] (e.g., migraine headaches, stroke, brain cancer, etc.), and even lung cancer.[9,10] In addition, during the biosynthesis of thiol-containing amino acids (such as cysteine and glutathione), SO_2 can be generated in biological systems.[11,12] However, the potential physiological properties of SO_2 and its derivatives are unknown. Therefore, it is of great importance to develop effective methods for detection of SO_2 and its derivatives in medical diagnosis and disease research.

Several analytical methods including spectrophotometry,[13] high-performance liquid chromatography (HPLC),[14] electrochemistry,[15] piezoelectric sensor,[16] and capillary electrophoresis[17] have been used to detect SO_2 and its derivatives. However, these methods require complicated operation and need destructive samples, although they offer high sensitivity and selectivity to sulfur dioxide. On the other hand, fluorescence imaging is one of the most attractive techniques due to its advantages in terms of real-time detection, convenient sample preparation, and spatial resolution.[18−20] So far, a number of fluorescent probes for the detection of sulfite (or bisulfite) have been reported.[21−25] Nevertheless, several challenges for detecting sulfur dioxide still exist. First, most of the probes are usually excited by one-photon (OP) and short

emission wavelengths (<600 nm), possessing shallow penetration compared with two-photon (TP) and deep-red emission modes,[26] which may limit their further applications in living biological systems. Second, some probes have relatively small emission shifts, which are unfavorable for detecting ratios because of the spectral overlap between the probes and the products after interaction with analytes. Furthermore, the response time of some probes is too long to constrict their desirable applications. Therefore, it is necessary to develop new TP and deep-red emission probes with a large emission shift for rapid detection of sulfite (or bisulfite) in living systems.

Herein, we describe a novel TP ratiometric fluorescent probe for sulfite based on the Michael-Addition reaction. The structure of the new probe is a coumarin π-conjugated system with emission at 645 nm, and HSO_3^- can interrupt the π-conjugated system via the Michael-Addition reaction. As a result, the emission of coumarin (450 nm), which is a typical TP fluorophore, would be obtained. Therefore, the unique probe can satisfy the need for imaging sulfite (or bisulfite) in TP and deep-red emission modes. Moreover, the novel probe showed ultrafast response to bisulfite (in less than 5 s) with a great emission shift and large emission signal ratios. Importantly, the innovative probe was also successfully applied for detection of SO_2 not only in the mitochondria of living cells but also in brain tissues and zebrafishes.

■ EXPERIMENTAL SECTION

Materials and Instruments. Unless otherwise stated, ultrapure water was used in all experiments and all reagents were obtained from commercial suppliers without further purification. Solvents were purified by standard methods prior to use. The pH measurements were performed with a Mettler-Toledo Delta 320 pH meter. UV−vis absorption spectra were obtained on a Shimadzu UV-2700 spectrophotometer, and fluorescence spectra were measured on a HITACHI F4600 fluorescence spectrophotometer. MTT was purchased from J&K Scientific Ltd. Fluorescence imaging experiments were performed with Nikon A1MP confocal microscopy. TLC analysis was carried out on silica gel plates, and column chromatography was conducted over silica gel (mesh 200−300); both of them were purchased from the Qingdao Ocean Chemicals. ^{1}H and ^{13}C NMR spectra were measured on an AVANCE III digital NMR spectrometer, using tetramethylsilane (TMS) as internal reference. High resolution mass spectrometric (HRMS) analyses were measured on an Agilent 1100 HPLC/MSD spectrometer.

General Procedure for Spectral Measurements. The stock solution of the two-photon (TP) and deep-red emission ratiometric fluorescent probe (**CP**) (1 mM) was prepared in DMSO. The various testing analytes stock solutions (Hcy, GSH, Cys, H_2O_2, NaClO, KI, NaN_3, NaF, *tert*-Butyl hydroperoxide (TBHP), $Na_2S_2O_3$, CH_3COONa, KSCN, sodium nitroprusside (releasing agent of NO), $FeSO_4$, $MgCl_2$, $ZnCl_2$, $CaCl_2$, $NaNO_3$, $NaHSO_3$, Na_2SO_3, Na_2SO_4, $NaNO_2$) were prepared at 100 mM in twice distilled water, and the *ditert*-butylperoxide (DTBP) stock solution (100 mM) was prepared in the DMSO. The test solution contained **CP** (5.0 μM), PBS buffer (pH 7.4, 10 mM, 5% DMSO), and 100 equiv of each analyte. Then, the absorption and fluorescence spectra were measured.

Cytotoxicity Assays. The cytotoxicity of **CP** to HeLa cells was studied by standard MTT assays. Two × 10^4 cells/mL HeLa cells were seeded in 96-well plates and then incubated with various concentrations of **CP** (0−20 μM) for 24 h. After that, 10 μL of MTT (5 mg/mL) was added to each well. After being incubated for 4 h, the supernatants were aspirated and 100 μL of DMSO was added. The absorbance of the solution at 570 nm was recorded using a microplate reader. The cell viability (%) = $(OD_{sample} − OD_{blank})/(OD_{control} − OD_{blank}) ×$ 100%.

Cell Culture and Fluorescence Imaging. HeLa cells were cultured in Dulbecco's Modified Eagle media (DMEM, Hyclone) supplemented with 10% fetal bovine serum (FBS, Sijiqing), penicillin (100 U/mL, Hyclone), and streptomycin sulfate (100 U/mL, Hyclone) under an atmosphere of 5% CO_2 and 95% air at 37 °C.

Before the imaging experiments, HeLa cells were seeded in confocal plates (2 × 10^4 cells/mL). After 24 h, the cells were pretreated with 10 μM NaHSO$_3$ for 30 min and then incubated with **CP** (5 μM) for 30 min at 37 °C. Cell imaging was performed after the cells were washed twice with PBS. Fluorescence images were acquired with a Nikon A1R confocal microscope with a 40× objective lens. The OP fluorescence excited at 405 nm for the blue channel (425−475 nm) and at 561 nm for the red channel (570−620 nm). The TP fluorescence emission was collected at blue and red channels upon excitation at 760 nm.

Fluorescence Imaging of Sulfur Dioxide Derivatives in Brain Slices. Rat brain slices were prepared from the brain of 4-weeks-old living Balb/c mice, which was approved by the Animal Ethical Experimentation Committee of Shandong University. The fresh brain tissues were incubated with 20 μM NaHSO$_3$ for 30 min, and then, 10 μM **CP** was added for another 30 min. Before imaging, the tissues were washed with PBS three times. A Nikon A1R confocal microscope with a 40× objective lens was used for fluorescence images. All of these experiments meet the relevant laws and institutional guidelines.
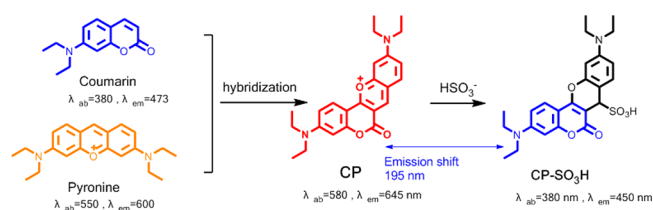
Fluorescence Imaging of Sulfur Dioxide Derivatives in Zebrafishes. Wild type zebrafishes were obtained from the Nanjing Eze-Rinka Biotechnology Co., Ltd. 3-day-old zebrafishes were transferred into confocal plates, and 20 μM NaHSO$_3$ was fed for 30 min; then, 10 μM **CP** was added and further incubated for another 30 min. After that, the zebrafishes were transferred into new glass bottom dishes for imaging. Fluorescence images were acquired with a Nikon A1R confocal microscope with a 4× objective lens. The excitation and emission wavelengths were the same as for fluorescence imaging in living cells.

Synthesis of CP. 4-Chloro-7-diethylaminocoumarin-3-aldehyde (**3**) (0.28 g, 1 mmol) and 3-diethylaminophenol (0.198 g, 1.2 mmol) were added to acetic acid (5 mL) and refluxed for 3 h. After cooling to room temperature, 70% perchloric acid (2.0 mL) was added to the mixture. A deep purple powder solid was precipitated by the dropwise addition of water, and then, the precipitate was filtered. The crude product was further purified by flash chromatography to afford a purple solid, 0.15 g with a yield of 50%. ^{1}H NMR (400 MHz, DMSO-d_6, δ) 8.95 (s, 1H), 8.05 (t, J = 9.2 Hz, 2H), 7.40 (dd, J_1 = 9.6 Hz, J_2 = 2.4 Hz, 1H), 7.33 (d, J = 1.8 Hz, 1H), 7.06 (dd, J_1 = 9.6 Hz, J_2 = 2.4 Hz, 1H), 6.08 (d, J = 2.0 Hz, 1H), 3.75 (q, J = 6.8 Hz, 4H), 3.62 (q, J = 7.2 Hz, 4H), 1.26 (m, 6H), 1.20 (t, J = 6.8 Hz, 6H); ^{13}C NMR (100 MHz, DMSO-d_6, δ) 162.40, 158.25, 158.02, 157.82, 157.76, 155.70, 144.03, 134.15, 128.39, 116.62, 116.30, 112.18, 104.49, 100.43, 98.88, 97.42, 77.24, 65.33, 45.85, 12.62. HRMS (*m/z*): [M + H]$^+$ calcd for $C_{24}H_{27}N_2O_3^+$, 391.2016; found, 391.2005.

■ RESULTS AND DISCUSSION

Design and Synthesis of CP. The rigid hybridization of two classical dyes is a robust strategy for development of effective long-wavelength dyes.[27,28] Long-wavelength dyes have several advantages, such as favorable photostability and high fluorescence quantum yields. It is known that benzopyrylium unit as a receptor can be attacked by SO_2.[23] On the basis of this consideration, we constructed a novel fluorescent probe (**CP**; Scheme 1) which was designed by hybridization of coumarin and pyroine moieties. We anticipated that $HSO_3^−$ ions might interrupt the coumarin-benzopyrylium π-conjugated system

Scheme 1. Design of the Two-Photon Ratiometric Fluorescent Probe CP

and thereby afford the optical profile of the coumarin dye. The synthetic route of **CP** was developed as shown in Scheme S1. Condensation of malonic acid and phenol in $POCl_3$ gave compound **1** in 98% yield, which was then mixed with 3-*N*,*N*-diethylaminophenol to afford compound **2**. Under nitrogen, compound **2** was stirred in DMF and $POCl_3$ to afford the key intermediate **3**. Finally, **CP** was obtained by condensation of **3** with 3-diethylaminophenol in acetic acid (yield: 50%). The structure of the intermediate **3** was confirmed by ^1H NMR, and the probe **CP** was fully characterized by ^1H NMR, ^{13}C NMR, and HRMS.

Optical Properties of the Probe CP. With the probe in hand, we performed the titration of **CP** in the absence or presence of SO_2 in phosphate buffer (pH 7.4, 10 mM, 5% DMSO). As shown in Figure 1, the free probe displayed a
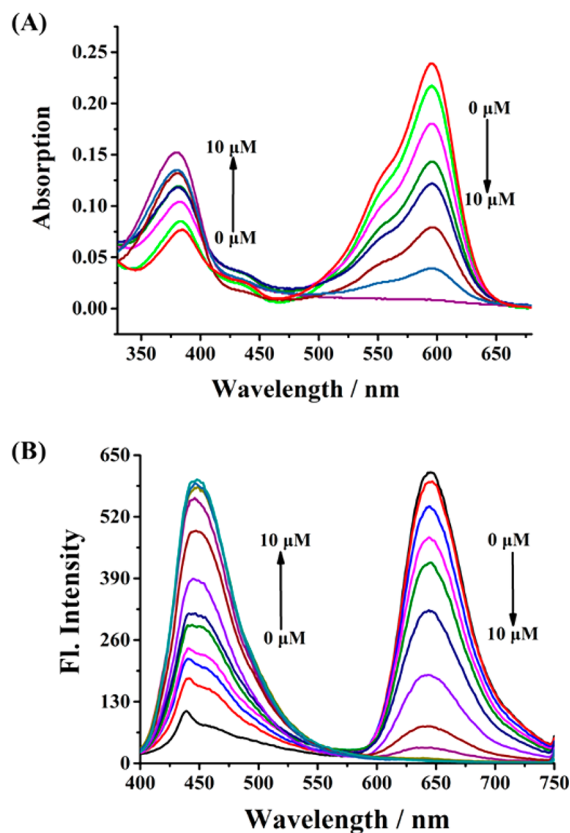

Figure 1. Absorption (A) and fluorescence (B) of the two-photon ratiometric fluorescent probe **CP** (5 μM) upon addition of various concentrations of $NaHSO_3$ (0−10 μM) in phosphate buffer (pH 7.4, 10 mM, 5% DMSO). λ_{ex} = 380 nm.

maximal absorption at around 580 nm. As designed, the free probe **CP** (5 μM) exhibited a strong emission spectra at 645 nm (Figure 1B). Satisfactorily, upon the addition of $NaHSO_3$ (0−10.0 μM), a progressive decrease at 580 nm absorbance peak and a gradual increase at around 380 nm (Figure 1A) were obtained. In addition, the fluorescence intensity of the **CP** displayed a distinct decrease at 645 nm and a gradual increase at 450 nm upon the excitation at 380 nm (Figure 1B), which is consistent with the variation of absorption spectrum. Furthermore, when excited at 580 nm, the fluorescent intensity at 645 nm was gradually decreased with the addition of different concentrations of $NaHSO_3$ (Figure S1). Notably, the two emission bands were well-separated at 450 and 645 nm,

making a large blue-emission shift of 195 nm which far exceeds the emission shift of the reported ratiometric SO_2 probes (Table S1). This large blue-emission shift (195 nm) could be due to the unique nucleophilic addition reaction at the benzopyrylium moiety by HSO_3^-, which interrupts the coumarin π-conjugated system. Thereby, the blue-emission of coumarin chromophore was obtained. In addition, the fluorescence intensity ratio (I_{450}/I_{645}) was saturated after adding 2 equiv of $NaHSO_3$ and increased from 0.1347 to 100.14. It is worth noting that such a dramatic signal ratio variation is highly sought. The I_{450}/I_{645} value is also proportional toward $NaHSO_3$ concentrations in the range from 0.5 to 1.5 μM with a detection limit of 0.39 μM (Figure S2). These favorable results suggest that **CP** may potentially be applied for detection of SO_2.

In order to verify the reaction mechanism of **CP** toward SO_2, the reaction product was characterized by ESI-MS. As shown in Figure S3, when **CP** was treated with $NaHSO_3$, a prominent peak at m/z 471.1580 $[M − H]^-$ was observed, which correspondings to **CP-SO₃H** (the probe−HSO_3^- adduct) (calcd 471.1595 for $C_{24}H_{28}N_2O_6S$). Furthermore, as afore-mentioned, upon addition of $NaHSO_3$, a distinct blue shift in both the absorption and emission was displayed. Thus, the results of HR-MS and spectral studies are in good agreement with the proposed mechanism in Scheme 1.

The kinetic ratio profiles (I_{450}/I_{645}) of **CP** (5 μM) toward the SO_2 were displayed in 10 mM PBS buffer at pH 7.4. As shown in Figure 2, upon introduction of $NaHSO_3$, the ratios
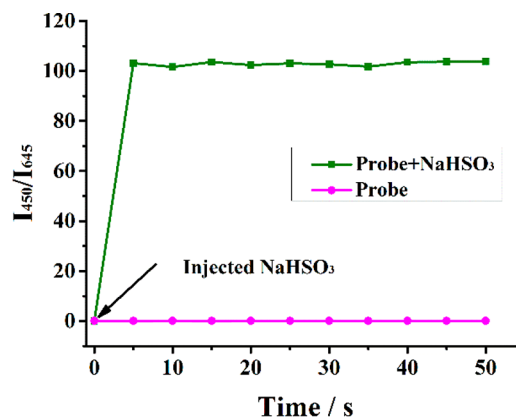

Figure 2. Time-dependent ratio intensities (I_{450}/I_{645}) of **CP** (5 μM) in the absence or presence of $NaHSO_3$ (5 μM) in phosphate buffer (pH 7.4, 10 mM, 5% DMSO). λ_{ex} = 380 nm.

immediately reached an equilibrium intensity in a very short time (in less than 5 s) and maintained stability. The response of **CP** toward $NaHSO_3$ is so fast that we could not test the equilibrium time. From the movie (in the Supporting Information), we can see that the solution showed a remarkable change after the addition of $NaHSO_3$ within 5 s. These results suggested that **CP** can respond to SO_2 in ultrafast fashion. In addition, the reaction solutions of **CP** in the absence or presence of SO_2 were successively irradiated for over 60 min, and the results implied that the probe has good photostability (Figure S4) and was irreversible to SO_2 (Figure S5).

To further gain insight into the selectivity of the probe **CP** toward SO_2 derivatives, some representative cations (Zn^{2+}, Mg^{2+}, Fe^{2+}, Na^+, K^+, Ca^{2+},), anions (NO_2^-, NO_3^-, N_3^-, SCN^-, SO_4^{2-}, $S_2O_3^{2-}$, SO_3^{2-}, HSO_3^-, CH_3COO^-, Cl^-, F^-, I^-),

reactive oxygen species (H_2O_2, NaClO, *tert*-butyl hydroperoxide (TBHP), *ditert*-butyl peroxide (DTBP)), biothiols (Cys, GSH, Hcy), and reactive nitrogen species (NO) were treated with **CP** in PBS buffer. As shown in Figure 3, only
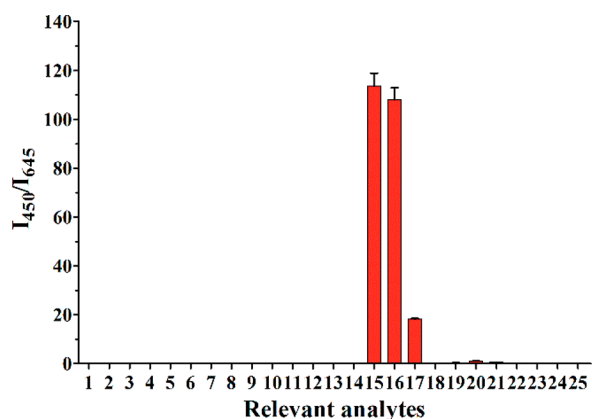

Figure 3. Fluorescent ratio (I_{450}/I_{645}) of the probe **CP** (5 μM) to various relevant analytes in phosphate buffer (pH 7.4, 10 mM, 5% DMSO). 1, only the probe **CP**; 2, $CaCl_2$; 3, $ZnCl_2$; 4, $MgCl_2$; 5, KI; 6, NaF; 7, $NaNO_2$; 8, $NaNO_3$; 9, NaN_3; 10, KSCN; 11, Na_2SO_4; 12, $FeSO_4$; 13, NaOAc; 14, $Na_2S_2O_3$; 15, $NaHSO_3$; 16, Na_2SO_3; 17, NaHS; 18, NO; 19, Cys; 20, GSH; 21, Hcy; 22, H_2O_2; 23, TBHP; 24, DTBP; 25, NaClO. λ_{ex} = 380 nm.

Na_2SO_3 and $NaHSO_3$ induced large ratiometric (I_{450}/I_{645}) fluorescence changes. Other biologically relevant molecules did not show obvious ratiometric fluorescence changes. These results showed that the new ratiometric fluorescence probe **CP** can detect SO_2 derivatives selectively.

We then examined the fluorescence profiles of **CP** in the absence or presence of $NaHSO_3$ at different pH values. As shown in Figure S6, **CP** is stable in the pH range from 4 to 9. In contrast, in the presence of HSO_3^-, a distinct fluorescent ratio increase was observed for the pH range of 4−6, with the maximum change at pH 5. To some extent, this is due to the concentration of HSO_3^- being directly related to the change of fluorescence intensity. HSO_3^- is the main nucleophilic ion and it exists solely at pH 5.0, while at pH 7.4, HSO_3^- and SO_3^{2-} are the major forms.[29]

Fluorescence Imaging of SO_2 in Living Cells. Encouraged by the results of the above studies, we decided to further evaluate the capability of **CP** to detect SO_2 in living cells. Before proceeding with fluorescence imaging, we investigated the cytotoxicity of **CP** to HeLa cells with the standard MTT assays. The results showed that **CP** has low cytotoxicity to HeLa cells (Figure S7,) indicating the probe may be potentially suitable for imaging in living cells.

We reasoned that the probe may be accumulating in the mitochondria due to the overall positive charge nature of **CP**. Therefore, we first conducted the fluorescence colocalization studies, which involved simultaneously staining HeLa cells with **CP** and the commercial mitochondrial tracker Mito-Tracker Green. As shown in Figure 4, an evident overlap between the red fluorescence of **CP** and the green fluorescence of Mito-Tracker Green was observed. The variations in the intensity profiles of the linear regions of interest (ROI) across the cells in the two channels showed a tendency toward synchrony. Moreover, the Pearson's correlation coefficients were calculated as 0.90. These results confirmed that **CP** mainly accumulated in the mitochondria.
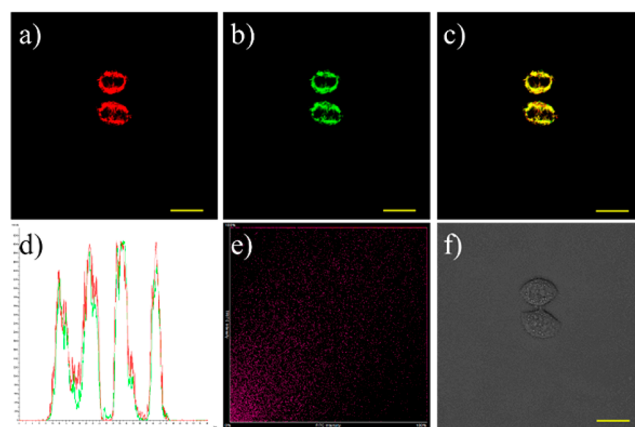

Figure 4. Images of the living HeLa cells costained with (a) 5 μM **CP** (λ_{ex} = 561 nm, λ_{em} = 570−620 nm) and (b) 0.2 μM Mito-Tracker Green (λ_{ex} = 488 nm, λ_{em} = 500−550 nm). (c) The merged pattern of (a) and (b). (d) Intensity profile of ROI across the cells in the red and green channels. (e) The intensity scatter plot of two channels. (f) Bright-field of HeLa cells. Scale bar: 20 μm.

Then, the effectiveness of **CP** for imaging SO_2 in HeLa cells was examined. The bright-field of the HeLa cells was shown in Figure S8. When incubated with 5 μM **CP** for 30 min, the HeLa cells mainly provided strong red fluorescence (Figure 5A). While the cells were pretreated with 10 μM $NaHSO_3$ for
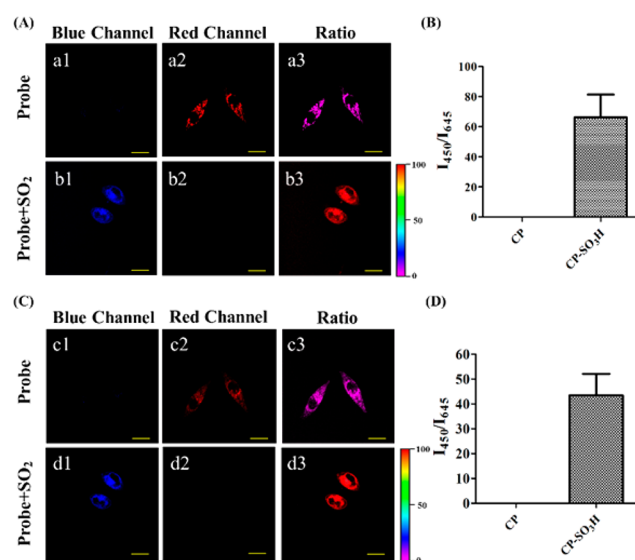

Figure 5. Fluorescence images of HeLa cells at one-photon (A) and two-photon (C) modes. (a1−a3) and (c1−c3) are the fluorescence images of HeLa cells treated with 5 μM **CP**. (b1−b3) and (d1−d3) are the fluorescence images of HeLa cells treated with 10 μM $NaHSO_3$ and then treated with 5 μM **CP**. Fluorescence images of HeLa cells at the blue channel (a1−d1) and red channel (a2−d2). Fluorescence ratio (a3−d3) images of blue channel and red channel. (B) and (D) are the ratios of I_{450}/I_{645} from (A) and (C). Scale bar: 20 μm.

30 min and then treated with 5 μM **CP** for another 30 min, the marked enhanced blue fluorescence was observed and simultaneously the red fluorescence was diminished at the OP mode. Meanwhile, the obvious (Figure 5C) blue fluorescence increase and red fluorescence decrease can also be noted at the TP mode. These studies showed that **CP** has a

good membrane permeability and can monitor SO_2 in living cells at deep-red and TP modes simultaneously.

Fluorescence Imaging of SO_2 in Brain Tissues. Epidemiological studies imply that SO_2 exposure can induce neurotoxicity and increase the risk of brain disorders.[30] Also, experimental studies suggest that SO_2 exposure was responsible for DNA breaks in brains of rats.[31] However, its detailed mechanisms remained unclear. It is of particular significance to detect SO_2 in brain tissues.

We thus further decided to use the probe to detect SO_2 in living brain tissues. As shown in Figure 6, the tissues treated
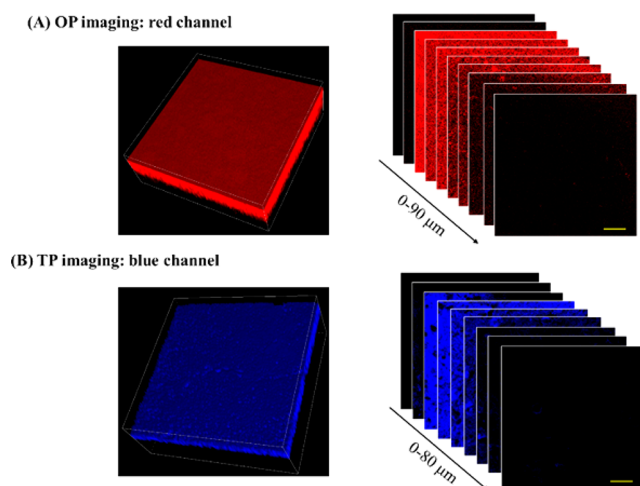

Figure 6. (A) **CP** 3D fluorescence images of the brain slices from mice in one-photon mode. λ_{ex} = 561 nm, λ_{em} = 570−620 nm. (B) 3D fluorescence images of brain tissue stained with 20 μM $NaHSO_3$ and 10 μM **CP** in two-photon mode. λ_{ex} = 760 nm, λ_{em} = 425−475 nm. Scale bar: 25 μm.

with 10 μM **CP** exhibited strong red fluorescence up to a penetration depth of 90 μm in the OP mode (Figure 6A). In contrast, the brain slices incubated with 20 μM $NaHSO_3$ for 30 min and then treated with 10 μM **CP** for another 30 min displayed obvious blue fluorescence with a depth of 80 μm in TP mode (Figure 6B). The above results showed that **CP** could image SO_2 in living brain tissues by deep-red and TP modes.

Fluorescence Imaging of SO_2 in Zebrafishes. Lately, zebrafishes are widely used as a vertebrate model for studying human genetic diseases due to their advantages of having a close homology to humans.[32,33] To further validate the simultaneous deep-red and TP imaging in vivo, we used zebrafish larvae as the vertebrate model. The bright-field of zebrafish larvae was shown in Figure S9. When zebrafish larvae were treated with 10 μM **CP** for 30 min, the strong red fluorescence was exhibited under OP excitation (Figure 7A). In comparison, $NaHSO_3$ pretreated with zebrafish larvae and further treated with **CP** induced a significant fluorescent emission in the blue channel and the red channel was diminished simultaneously under OP excitation. Notably, the same fluorescence changes of **CP** in response to SO_2 were also observed under TP excitation at 760 nm (Figure 7C). Thus, the in vivo study indicated that **CP** could readily enter zebrafishes and detect SO_2 effectively under OP and TP excitation.

CONCLUSION

In conclusion, we have constructed a new TP and deep-red emission ratiometric fluorescent probe **CP** based on the
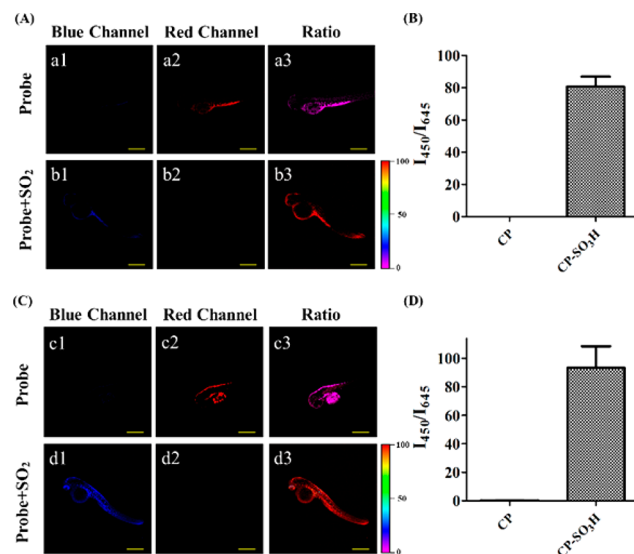

Figure 7. Fluorescence images of zebrafishes at one-photon (A) and two-photon (C) modes. (a1−a3) and (c1−c3) are the fluorescence images of zebrafishes treated with 5 μM **CP**. (b1−b3) and (d1−d3) are the fluorescence images of zebrafishes treated with 10 μM $NaHSO_3$ and then treated with 5 μM **CP**. Fluorescence images of zebrafishes at the blue channel (a1−d1) and red channel (a2−d2). Fluorescence ratio (a3−d3) images of blue channel and red channel. (B) and (D) are the ratios of I_{450}/I_{645} from (A) and (C). Scale bar: 500 μm.

nucleophilic addition reaction of SO_2 toward the electrically positive benzopyrylium moiety. The novel probe **CP** displayed ultrafast response to SO_2 in less than 5 s with a large blue-emission shift (195 nm) and exhibited a dramatic enhancement for the emission ratios from 0.1347 to 100.14. Importantly, **CP** can respond to SO_2 in the HeLa cells, brain tissues, and zebrafishes under OP and TP modes. The design of the unique SO_2 probe with ultrafast response and a large blue-emission shift presented herein may open a new avenue for the development of robust ratiometric fluorescent probes for exciting applications in medical diagnosis and disease research.

ASSOCIATED CONTENT

S **Supporting Information**

The Supporting Information is available free of charge on the ACS Publications website at DOI: 10.1021/acs.anal-chem.7b02216.

Synthesis of the probes, absorption and fluorescence spectra, imaging assays, and ^{1}H NMR and ^{13}C NMR spectra (PDF)

Movie showing the change in solution after the addition of $NaHSO_3$ (ZIP)

AUTHOR INFORMATION

Corresponding Author

*Fax: + 86-531-82769031. E-mail: weiyinglin2013@163.com.

ORCID

Yanyan Ma: 0000-0002-9358-5866

Yonghe Tang: 0000-0002-7282-4610

Weiying Lin: 0000-0001-8080-4102

Notes

The authors declare no competing financial interest.

REFERENCES

(1) Chen, T.; Gokhale, J.; Shofer, S.; Kuschner, W. *Am. J. Med. Sci.* **2007**, *333*, 249−256.

(2) Kampa, M.; Castanas, E. *Environ. Pollut.* **2008**, *151*, 362−367.

(3) Salurcan, A.; Türkyılmaz, M.; Özkan, M. *Food Chem.* **2017**, *221*, 412−421.

(4) Morgan, S.; Scholl, C.; Benson, N.; Stone, M.; Durall, D. *Int. J. Food Microbiol.* **2017**, *244*, 96−102.

(5) Nassar, R.; Trivella, A.; Mokh, S.; Al-Iskandarani, M.; Budzinski, H.; Mazellier, P. *J. Photochem. Photobiol., A* **2017**, *336*, 176−182.

(6) Pannullo, F.; Lee, D.; Neal, L.; Dalvi, M.; Agnew, P.; O'Connor, F.; Mukhopadhyay, S.; Sahu, S.; Sarran, C. *Environ. Health* **2017**, *16*, 29.

(7) Smith, T.; Peters, J.; Reading, J.; Castle, C. *Am. Rev. Respir. Dis.* **1977**, *116*, 31−39.

(8) Sang, N.; Yun, Y.; Yao, G.; Li, H.; Guo, L.; Li, G. *Toxicol. Sci.* **2011**, *124*, 400−413.

(9) Beeson, W.; Abbey, D.; Knutsen, S. *Environ. Health. Perspect.* **1998**, *106*, 813−822.

(10) Lee, W.; Teschke, K.; Kauppinen, T.; Andersen, A.; Jäppinen, P.; Szadkowskastanczyk, I.; Pearce, N.; Persson, B.; Bergeret, A.; Facchini, L.; et al. *Environ. Health. Perspect.* **2002**, *110*, 991−995.

(11) Ubuka, T.; Ohta, J.; Yao, W.; Abe, T.; Teraoka, T.; Kurozumi, Y. *Amino Acids* **1992**, *2*, 143−155.

(12) Du, S.; Jin, H.; Bu, D.; Zhao, X.; Geng, B.; Tang, C.; Du, J. *Acta Pharmacol. Sin.* **2008**, *29*, 923−930.

(13) West, P.; Gaeke, G. *Anal. Chem.* **1956**, *28*, 1816−1819.

(14) Zhao, Y.; Qiu, W.; Yang, C.; Wang, J. *Energy Fuels* **2017**, *31*, 693−698.

(15) Yilmaz, U.; Somer, G. *Anal. Chim. Acta* **2007**, *603*, 30−35.

(16) Pundir, C.; Rawal, R. *Anal. Bioanal. Chem.* **2013**, *405*, 3049−3062.

(17) Palenzuela, B.; Simonet, B.; Ríos, A.; Valcárcel, M. *Anal. Chim. Acta* **2005**, *535*, 65−72.

(18) Raue, R. *Methine Dyes Pigm.* **2000**, DOI: 10.1002/14356007.a16_487.

(19) Daehne, S., Resch-Genger, U., Wolfbeis, O., Eds. *Near-Infrared Dyes for High Technology Applications*; Kluwer: Boston, 1998; Vol. 52.

(20) He, L.; Dong, B.; Liu, Y.; Lin, W. *Chem. Soc. Rev.* **2016**, *45*, 6449−6461.

(21) Liu, X.; Yang, Q.; Chen, W.; Mo, L.; Chen, S.; Kang, J.; Song, X. *Org. Biomol. Chem.* **2015**, *13*, 8663−8668.

(22) Chen, W.; Fang, Q.; Yang, D.; Zhang, H.; Song, X.; Foley, J. *Anal. Chem.* **2015**, *87*, 609−616.

(23) Chen, Y.; Wang, X.; Yang, X.; Zhong, Y.; Li, Z.; Li, H. *Sens. Actuators, B* **2015**, *206*, 268−275.

(24) Wang, C.; Feng, S.; Wu, L.; Yan, S.; Zhong, C.; Guo, P.; Huang, R.; Weng, X.; Zhou, X. *Sens. Actuators, B* **2014**, *190*, 792−799.

(25) Zhang, H.; Xue, S.; Feng, G. *Sens. Actuators, B* **2016**, *231*, 752−758.

(26) Dong, B.; Song, X.; Kong, X.; Wang, C.; Tang, Y.; Liu, Y.; Lin, W. *Adv. Mater.* **2016**, *28*, 8755−8759.

(27) Bochkov, A.; Akchurin, I.; Dyachenko, O.; Traven, V. *Chem. Commun.* **2013**, *49*, 11653−11655.

(28) Chen, H.; Dong, B.; Tang, Y.; Lin, W. *Acc. Chem. Res.* **2017**, *50*, 1410−1422.

(29) Ropp, R. *Encyclopedia of the Alkaline Earth Compounds.* **2013**, 1179−1187.

(30) Hong, Y.; Lee, J.; Kim, H.; Kwon, H. *Stroke* **2002**, *33*, 2165−2169.

(31) Meng, Z.; Qin, G.; Zhang, B.; Bai, J. *Mutagenesis* **2004**, *19*, 465−468.

(32) Poss, K.; Wilson, L.; Keating, M. *Science* **2002**, *298*, 2188−2190.

(33) Laughlin, S.; Baskin, J.; Amacher, S.; Bertozzi, C. *Science* **2008**, *320*, 664−667.